ADVANCED FUNCTIONAL MATERIALS
www.afm-journal.de
Materials Views
www.MaterialsViews.com

Water-Based Isotropically Conductive Adhesives: Towards Green and Low-Cost Flexible Electronics

Cheng Yang, Wei Lin, Zhongyu Li, Rongwei Zhang, Haoran Wen, Bo Gao, Guohua Chen, Ping Gao, Matthew M. F. Yuen,* and Ching Ping Wong**

This paper reports the first high-performance water-based isotropically conductive adhesives (WBICAs) – a promising material for both electrical interconnects and printed circuits for ultralow-cost flexible/foldable printed electronics. Through combining surface iodination and in situ reduction treatment, the electrically conductivity of the WBICAs are dramatically improved (8×10^{-5} Ω cm with 80 wt% of silver); moreover, their reliability (stable for at least 1440 h during 85 °C/85% RH aging) meets the essential requirements for microelectronic applications. Prototyped applications in carrying light emitting diode (LED) arrays and radio frequency identification (RFID) antennas on flexible substrates were demonstrated, which showed satisfactory performances. Moreover, their water-based character may render them more environmentally benign (no volatile organic chemicals involved in the printing and machine maintenance processes), more convenient in processing (reducing the processing steps), and energy economic (thermally sintering the silver fillers and curing the resin is not necessary unlike conventional ICAs). Therefore, they are especially advantageous for mass-fabricating flexible electronic devices when coupled with paper and other low-cost substrate materials such as PET, PI, wood, rubber, and textiles.

1. Introduction

Recently, there have been intensive studies into flexible electronic devices involving low materials cost, low processing temperature, high fabrication speed, and amenability to mass manufacturing (e.g., by reel-to-reel printing).[1–6] Technical improvements in these areas involve not only the development of organic and quantum electronic devices, but also the current surface-mounting technique (SMT) as the so-called "Chip-on-Flex" etc.[2,4] As basic components, printed electrical conductors and interconnects have been intensively studied in recent years so as to cater to the next generation of consumable flexible electronic devices.[7–10] Breakthroughs in these areas will benefit the development of many current consumer electronics including flexible displays,[4,11,12] flexible and conformal antenna arrays, thin film transistors,[13–16] membrane keyboards, electronic solar cell arrays,[17,18] radio-frequency identification (RFID) tags,[19] flexible batteries,[20,21] electronic circuits fabricated in e.g. clothing and biomedical devices etc.;[8,22–24] they will also enable a broad range of devices and applications that are not possible today.[25]

Conventional printed circuits and electrical interconnects are composed of the electrochemically etched copper foils and eutectic Sn/Pb solders.[26] Albeit the many advantages that they take, the high processing temperature and environmental cost, and the low fabrication speed still hurdle their broader applications in the future flexible electronic applications.[27] Recently, isotropically conductive adhesives (ICAs) have been intensively studied, which show great promise in substituting the above two categories of materials.[26,27] ICAs, the polymer composite materials with electrically conductive fillers, possess many characters such as low processing temperature and good printing resolution, and are compatible with conventional printing methods.[28] For example, ICAs can be printed through many conventional printing methods, and cured at 150 °C within a few minutes; in comparison, conventional lead-free solder materials reflow at temperatures typically higher than 250 °C. Thus ICAs help to simplify the processing steps and broaden the choices to

Prof. C. Yang
Division of Energy & Environment
Graduate School at Shenzhen
Tsinghua University
2279 Li Shui Road, Shenzhen, Guangdong Province, P. R. China
E-mail: yang.cheng@sz.tsinghua.edu.cn

Prof. C. Yang, H. Wen, B. Gao, Prof. M. M. F. Yuen
Department of Mechanical Engineering
The Hong Kong University of Science and Technology
Clear Water Bay, Hong Kong, P. R. China
E-mail: meymf@ust.hk

Prof. C. Yang, W. Lin, Dr. R. Zhang, Prof. C. P. Wong
School of Materials and Engineering
Georgia Institute of Technology
771 Ferst Drive, Atlanta, GA, 30332-0245, USA
E-mail: cp.wong@mse.gatech.edu

Dr. Z. Li, Prof. G. Chen, Prof. P. Gao
Department of Chemical and Biomolecular Engineering
The Hong Kong University of Science and Technology
Clear Water Bay, Hong Kong, P. R. China

DOI: 10.1002/adfm.201101433

© 2011 WILEY-VCH Verlag GmbH & Co. KGaA, Weinheim

low-cost substrate materials such as polyethylene terephthalate (PET) films.[5] Conventionally, bisphenol-A type of epoxies such as Shell® EPON 828 have been most studied as the resin material for the ICAs because of their high mechanical strength, good adhesion, thermal stability, and excellent reliability.[26,27,29] However, the possible release of bisphenol-A derivatives and toxic curing agents has become a serious concern for human health.[30] Moreover, a thermal curing process after printing is necessary to improve the electrical conductivity, mechanical strength, and reliability.[31,32] Alternatively, there are room-temperature-curable epoxy formulations and UV-curable free-radical-polymerization based acrylic resins; yet they face the problems such as the toxicity of the amino-curing agents, the relatively short shelf-life and oxidation issue due to free-radicals. To improve the performances (e.g. electrical conductivity and reliability) of various ICAs and reduce cost, a series of methods have been developed.[26,27] For example, nano-sized silver fillers have been added into the ICA formulations to enable the metallic fillers to sinter at lower temperature (<200 °C), as a result of the melting point depression effect. The sintering of metallic fillers reduces the contact resistance and improves the electrical conductivity of ICAs effectively.[28,33–37] Chemical modifications of the metallic fillers have been also proved effective to improve the electrical conductivity.[34] In particular, research into highly conductive ICAs with biocompatible and environmentally benign resin materials has attracted more attention in the recent years.[29,36,38,39]

Here we introduce the water-based ICAs (WBICAs) as an excellent alternative to the conventional oil-soluble ones. The WBICAs are composed of silver microflakes and water-based aliphatic polyurethane (PU) resin dispersant. Compared to the other traditional dispersants for ICAs, such as epoxy, polyester, and polyacrylate etc., water-based PU as the resin shows a few advantages. First, it is environmentally friendly. It is dispersed in water, and the manipulation does not involve toxic volatile materials. Moreover, the screen mash and stencil plate for printing the WBICAs can be conveniently cleansed by water after each printing cycle. Second, the mechanical strength of PU can be conveniently adjusted by choosing from a large pool of starting materials, even from the extractions of plants.[40,41] Third, the urethane bond is relatively strong, thus the materials have a high reliability for general electronic packaging applications. Forth, it is energy-economic. The curing step for the ICAs can take place even at room temperature (of course a higher temperature may help accelerate the process). Fifth, the rheological property of the WBICAs can be adjusted by controlling the water content, thus they are compatible to many conventional printing conditions such as screen printing, gravure printing, and roll-to-roll printing etc. Owning to all these advantages, the WBICAs are especially effective for mass fabricating/manufacturing flexible printed electronics on various ubiquitous substrate materials to maximize cost-effectiveness and find novel applications.

In order to improve the electrical conductivity of silver fillers, we combine surface iodination treatment[33] and in situ reduction treatment by adding a small dose of sodium borontetrahydride ($NaBH_4$).[42,43] Here, we discuss the relationship between the surface treatment conditions and the corresponding performances of the WBICAs, namely electrical conductivity and mechanical strength. We prototype and evaluate their applications in printed RFID antennas and circuits for supporting light-emitting diode (LED) chips on various ubiquitous substrates.

2. Results and Discussions

Recently, Yang et al. conducted investigations of end-group blocked polyurethanes (PUs) as a resin for ICAs.[44,45] PUs have been widely applied in coating and sealant industry,[42] which display a few characters including the adjustable mechanical properties, shape-memory property, environmentally benign character and excellent stability. They can be applied to various substrates and dried in ambient condition due to their unique water-based character. Moreover, many PU-based resins are biocompatible and can be obtained from renewable resources such as vegetable oils.[46–48] Taking all these advantages, here we investigate the feasibility of applying the water-based PU resin as the dispersant material for ICAs. Cycloaliphatic prepolymer is used here, which is characterized by the excellent reliability to UV irradiation. As shown in **Scheme 1**, the water-based PU

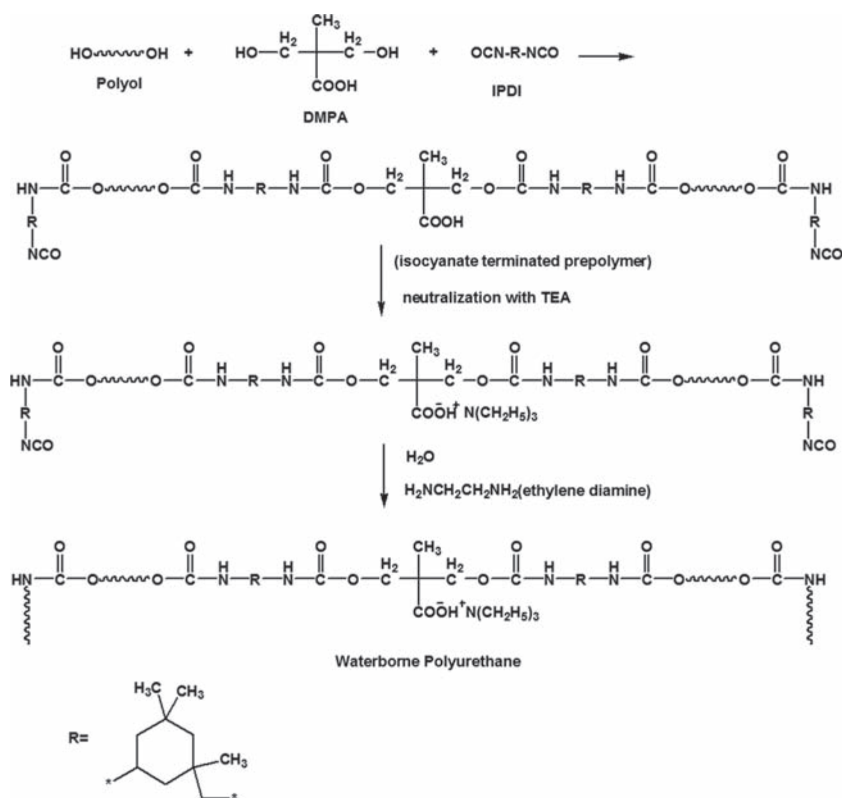

Scheme 1. The preparation route of the water-based PU dispersant for the ICAs.

© 2011 WILEY-VCH Verlag GmbH & Co. KGaA, Weinheim

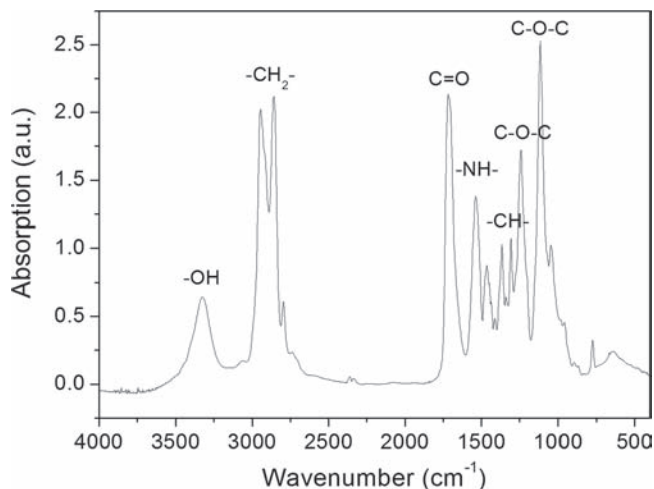

Figure 1. FT-IR spectrum of the dried film of the water-borne PU.

resin is prepared mainly in four steps according to the emulsion polymerization method:[49] 1) polyether diol, dimethylolpropionic acid (DMPA), and isophorone diisocyanate (IPDI) are mixed together for preparing the prepolymer; 2) chain extender (butylene diol) is added until the chain propagation is terminated; 3) triethylamine (TEA) is added to neutralize the system; 4) water is added dropwise under stirring to obtain the aqueous solution. The organic solvent (i.e. acetone in the lab condition) and the unreacted chemicals are removed by vacuum. The resulting translucent bluish PU emulsion has a long shelf-life and stable rheological property.

IPDI, a cycloaliphatic diisocyanate, is featured with the excellent mechanical strength and the reliability. Polyether diol (i.e. poly(tetrahydrofuran)-2000, PTHF 2000) is used as the curing agent which provides adequate moisture resistance, impact resistance and elastomeric character. DMPA is an ionic diol which assists the PU chains to be suspended in water due to the electrostatic interaction with the counter ions. Since it contains two primary hydroxyl groups (the same as PTHF 2000), so that the addition polymerization reaction between IPDI and PTHF and DMPA can take place with a similar velocity. Butylene diol is used to extend the chain length of the polymer to improve the mechanical property of the bulk polymer. The chemical structure and molecular weight of the PU resin was confirmed by FT-IR, ^{1}H-NMR, and GPC (See Supporting Information for details). As shown in **Figure 1**, the FT-IR spectrum of the dried film of the as-prepared water-based PU is investigated. The peak at 3324 cm^{-1} is attributed to the stretching of the hydroxyl group on the carboxylic acid; the peaks at 2933 cm^{-1} and 2854 cm^{-1} confirm the asymmetrical and symmetrical stretching of alkyl CH_2 group, the 1698 cm^{-1} the stretching of the carbonyl group, the peak at 1538 cm^{-1} confirms the vibration of -NH- amino group, the peaks at 1464 cm^{-1} and 1365 cm^{-1} confirms the scissoring and rocking of C-H group; and 1239 cm^{-1} and 1108 cm^{-1} confirm the stretching on the C-O-C group. The as-prepared PU has excellent thermal stability, which was confirmed by using thermal gravimetric analysis (TGA) in the air (**Figure 2**A). The weight loss is less than 10% at 250 °C, which may be related to the elimination of the triethylamine residue. Further raising the temperature led to the total decomposition and the decomposition finished at 430 °C. This result suggests that the PU dispersant is compatible with the general solder reflow process when it is applied in the conventional packaging process. Differencial scanning calorimetry (DSC) analysis of the PU sample (Figure 2B) suggests that the glass transition temperature (T_g) of the PU sample is at about −26.1 °C. The low T_g of this PU formulation renders superior flexibility at room temperature when WBICAs are used as thicker films.

The WBICAs were prepared by mixing the PU resin and the modified silver microflakes together in a THINKY ARE250 mixer.[41,50] By adjusting the ratio between the two components, we were able to achieve an optimum between the mechanical strength and the electrical conductivity. $NaBH_4$ has been considered as a very powerful reducing agent for protecting various metals from oxidation. Addition of a small amount of $NaBH_4$ has been demonstrated effective for improving the percolation among the copper and nickel powders via an in-situ reducing process for ink-jet printing conductive lines.[33] One mole of $NaBH_4$ is able to reduce four moles of silver oxide. However, an appreciable amount of $NaBH_4$ may slowly (and exothermically) react with water or alcohol to form sodium borate and hydrogen gas.

$$4Ag_2O + NaBH_4 \rightarrow 8Ag^0 + NaBO_2 + 2H_2O \quad (1)$$

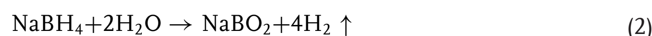

$$NaBH_4 + 2H_2O \rightarrow NaBO_2 + 4H_2 \uparrow \quad (2)$$

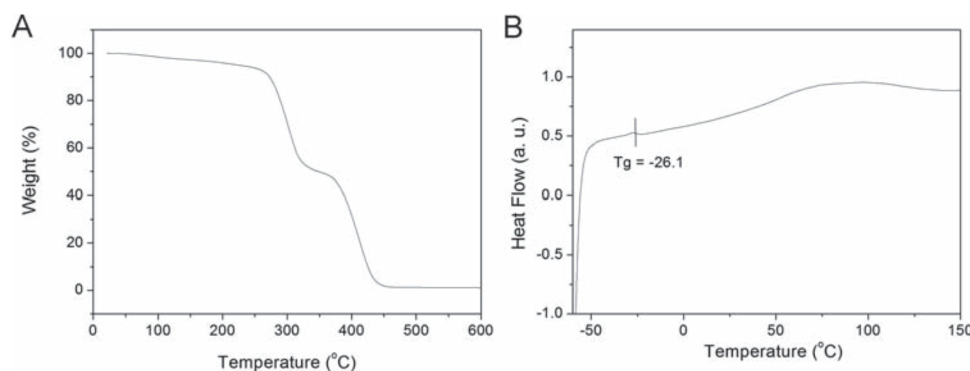

Figure 2. A) TGA analysis of the PU dried film. The sample was ramped from 25 °C to 600 °C in the air at 10 °C/min. B) DSC analysis of the PU dried film. The sample was ramped from −60 °C to 150 °C in the air at 10 °C/min.

© 2011 WILEY-VCH Verlag GmbH & Co. KGaA, Weinheim

Here we evaluated the influence of the addition of $NaBH_4$ towards a series of properties of the WBICAs by testing a series of different $NaBH_4$ concentrations. Concisely, 0.5 wt% and 1 wt% of $NaBH_4$ addition conditions were elucidated in details in this manuscript. Silver flakes used here were pretreated by an iodination step as previously reported;[33] the AgI nanoclusters at the silver flake surface were successfully transformed into Ag nanoparticles by the added $NaBH_4$ in a way similar to that of silver oxide.[51] The addition of $NaBH_4$ caused color change of the silver flakes, which renders them turning from the lustrous grey color to pale brown.[52] According to the work by Yang et al., the iodination pre-treatment of silver results in the formation of the nonstoichiometric Ag/AgI nanostructures at the surface of the silver flakes.[33,53] The addition of $NaBH_4$ caused the reduction of the Ag^+; thus the surface of the silver flakes formed Ag^0 nanostructures.[36,51,52] The freshly reduced silver nanostructures at the silver flakes may play a subtle role for the in-situ connections among the silver flakes. Sample cross sections were analyzed by the scanning electron microscopy (See Supporting Information for details).

The surface of the treated silver flakes was studied by surface-enhanced Raman spectroscopy (SERS). **Figure 3** displays the SERS spectra of Rhodamine 6G (R6G) on the surface-modified silver samples. The samples include: original silver flake sample; iodine treated silver sample; 0.5% $NaBH_4$-treated iodinated silver flake sample, and the 1% $NaBH_4$ treated iodinated silver flake sample. From the spectra, we can observe that the spectrum of the 1% $NaBH_4$ treated iodinated silver flake sample is dominated by the strong peaks at 1651, 1576, 1512, 1365, 1312, 1161, 1127, 775, and 614 cm^{-1}, which agreed with the previous report; meanwhile, the assignments have been well documented in the literature.[51,54] The result suggests that the contact between the R6G molecule and the substrate might be through xanthene groups and probably in end-on configuration. For the sample of the 0.5% $NaBH_4$ treated iodinated silver flakes, the signals of the above peaks are much weaker, which suggests a relatively weak SERS enhancement effect from the silver flakes in this treatment condition. However, from the spectra of the just-iodinated and the original silver flake samples, we didn't observe any SERS signal from R6G. In spectra **A** and **B**, the peaks originated from the carboxylic acid based lubricant are present in the original untreated silver flake samples (the symmetric (COO^-) stretching at 1432 cm^{-1} (or 1438 cm^{-1}) and asymmetric (COO^-) stretching at 1591 cm^{-1} (or 1587 cm^{-1})).[55–57] Additionally, the peak at 521 cm^{-1} in spectrum **A** originates from the silicon substrate.

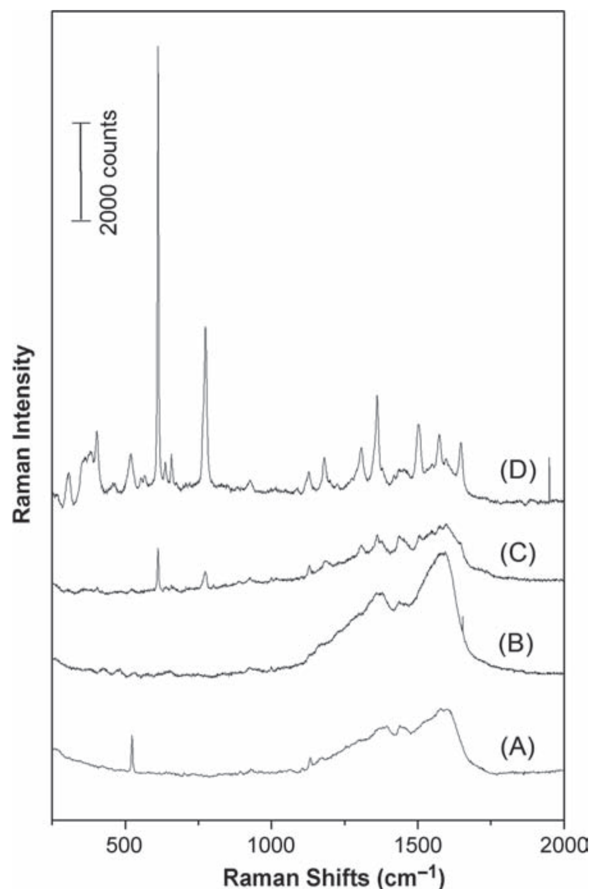

Figure 3. Raman scattering of the silver flake samples with the chemisorbed R6G. A) original silver flake sample; B) iodine treated silver sample; C) 0.5% $NaBH_4$ treated iodinated silver flake sample, and D) 1% $NaBH_4$ treated iodinated silver flake sample.

The main origin of the Raman enhancement observed for the $NaBH_4$-treated iodinated silver flakes is due to the surface plasmon resonance of the silver nanostructures formed by the $NaBH_4$ reduction treatment after the iodination treatment. Because of the mild iodination treatment condition, the silver nanostructure formed by the iodination/reduction process is a very thin layer, which is not able to be detected by XRD or observed clearly in SEM; whereas the strong SERS enhancement effect verifies the existence of such in-situ formed silver nanostructure, which agrees very well with the report by Nie et al.[53,58,59] The formation of the nanostructures may also explain the characteristic absorption band in the UV-vis spectra (See Supporting Information). The localized surface plasmon resonance modes created by strong electromagnetic coupling between the rims and surfaces of the nanostructures among the touching silver flakes are able to play a key role in surface enhancement, which was well explored as the "hot spots".[60]

Figure 4A shows the experimental results of the electrical resistivity data which were lower than 0.01 $\Omega \cdot$cm. As shown here, we can observe that the addition of $NaBH_4$ in the treatment of the silver flakes reduces the electrical resistivity of the printed WBICA resistors. Reduction by one order of magnitude in resistivity is achieved by using $NaBH_4$ treated iodinated silver flakes. The WBICA samples without the reduction treatment have a relatively high electrical resistivity (>0.01 $\Omega \cdot$cm) when the silver content is lower than 75% by weight; while the WBICA samples with the reduction treatment can still achieve a good electrical resistivity (<10^{-3} $\Omega \cdot$cm) when the silver content is higher than 65% by weight. This suggests that the silver nanostructure formed on the silver flake surface during the reduction treatment by $NaBH_4$ reduces the contact resistance between the silver flakes in the WBICA. Electrical resistivity of the WBICA samples with 85% filler loading level without either iodination or reduction treatment is higher than 1 $\Omega \cdot$cm (not shown in the figure). We carried out the temperature-humidity testing (THT) by monitoring the trend of the electrical resis-

© 2011 WILEY-VCH Verlag GmbH & Co. KGaA, Weinheim

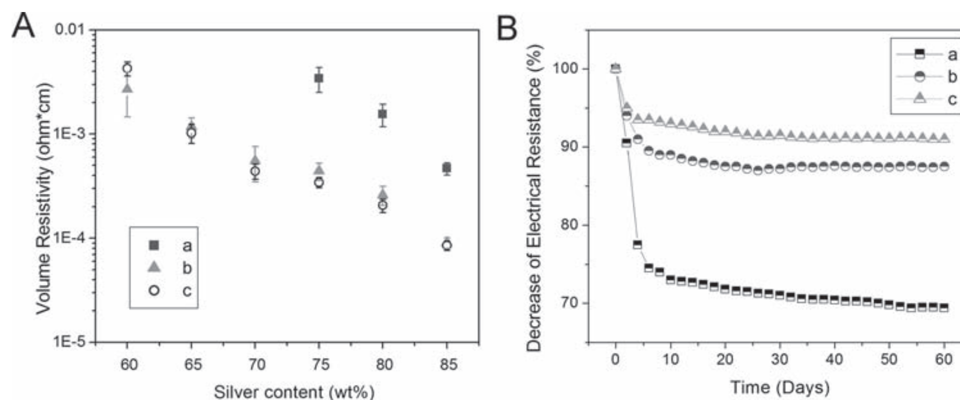

Figure 4. A) Volume resistivity of the WBICAs versus different addition amount of $NaBH_4$: a) no $NaBH_4$ addition; b) 0.5% of $NaBH_4$; c) 1% of $NaBH_4$. B) Temperature-humidity reliability of the WBICAs versus aging time: a) no $NaBH_4$ addition; b) 0.5% of $NaBH_4$; c) 1% of $NaBH_4$.

tivity of all printed resistor samples in a TERCHY MHU-150L humidity chamber (85 °C/85% relative humidity) for 1440 hours. As shown in Figure 4B, we can observe a trend of decrease of the electrical resistivity in the early few days, which is an interesting phenomenon that needs further explorations.[34] We also noted that the samples filled with the untreated silver flakes dropped about 30% in electrical resistance while the other two reduced silver flake filled WBICAs dropped less than 10%. Comparing the significant difference in the electrical resistivity of the reduced and unreduced samples (about one order of magnitude) after the THT testing, we confirm the significance of the addition of $NaBH_4$. After all, we did not observe any increase of the electrical resistivity of all samples after the aging test, which suggests sufficient reliability for real applications. For example, by simply applying a straight line of the WBICA (thickness ~20 μm; width ~2 mm) on a piece of stretchable natural rubber latex film (**Figure 5**), this WBICA based circuit can sufficiently support a few LED chips when a direct current (DC) is running through. Tensile test of the WBICA

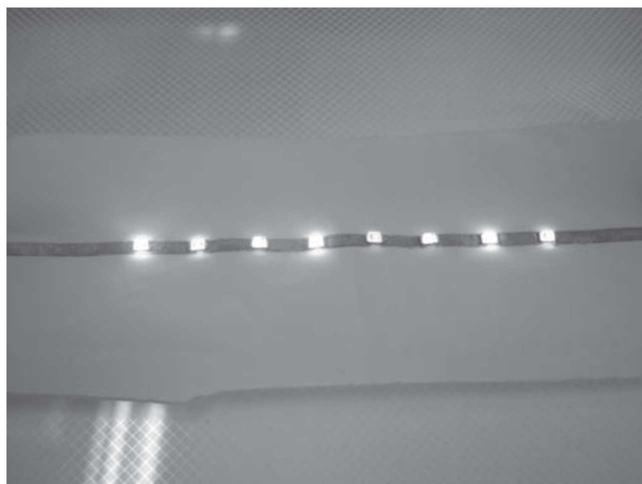

Figure 5. A photographic image of a piece of WBICA printed circuit line (2 mm x 150 mm) which supports 8 LED chips in different color. (Ag: 80 wt%, $NaBH_4$: 0.5%).

thin films suggested that they have excellent mechanical strength to cater to ubiquitous uses as the electrical circuits. (Table S1). Considering the relatively low high-temperature stability of many rubbery substrates, WBICAs may be an excellent choice as the circuits and interconnects for the low-cost stretchable electronics which are able to be fabricated at room temperature.

One of the immediate applications of the WBICAs is for printing the radio frequency identification (RFID) tag antennas. RFID technique is used for identifying and tracking items using radio waves, which has dramatically grown up in recent years and will gradually replace the traditional universal product code (UPC) barcodes to cater for the supply chain management in various commodities (such as food and garments supply chains).[61] Therefore, there are both the requirements of lower cost and lower environmental burden of the growing RFID market. The WBICA based RFID antennas may be a competitive alternative due to the convenience of processing and the green character.[62] Moreover, a large variety of substrate materials can be included to provide support of the WBICAs include papers, fabrics, PET films, wood etc., as shown in **Figure 6**, which is beneficial to the RFID applications (see Figure S4 for the antenna layout details). The signal transmittance performance of the RFID tags prepared based on the WBICAs is shown in **Figure 7**, which summarizes the read range performances and the corresponding electrical resistivity of some of the RFID tags with same geometry of antenna and same type of chips. It appears that the read range of all these RFID tags can reach to 7 meters, which were in the same level as compared to the oil-soluble counterparts.[63] The result suggests that the WBICAs are suitable for real applications of RFID antenna production.

3. Conclusions

In summary, we report the WBICA as a printed conductive material for some general applications in consumer flexible electronics. By sensitizing a small amount of $NaBH_4$ to the iodinated silver surface, it can effectively improve the bulk electrical conductivity by about one order of magnitude; the lowest

© 2011 WILEY-VCH Verlag GmbH & Co. KGaA, Weinheim

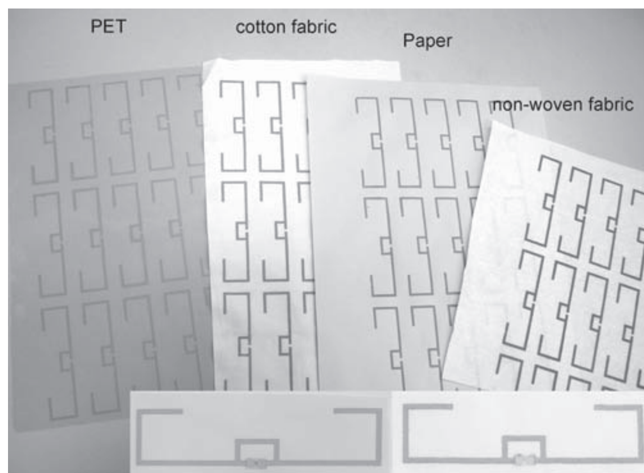

Figure 6. A photograph showing some of the RFID antennas which were printed on various substrate materials, including PET, cotton fabric, paper, and non-woven fabric. The two insets are the RFID tag samples on paper (left) and cotton fabric (right). The straps were attached to the antenna immediately after the antenna printing process.

electrical resistivity ever measured in this material was on the order of 10^{-5} Ω·cm. SERS analysis of the surface treated silver flakes suggests that the iodination/reduction treatment is able to generate pristine nanostructures which are able to promote electrical conductivity, the reason for which is still being explored. The thermal-humidity test results suggested that even though a large amount of water is involved in the synthesis and fabrication processes, it shows negligible concern for reliability. Due to the unique characters such as amenity for processing, environmentally benign character, highly conductive, excellent reliability and shelf-life etc., WBICAs may find an elegant balance point between the proof-of-concept flexible printed materials and modern electronic packaging technology. Moreover, due to the versatility of the prepolymers of PU, the mechanical behavior of the WBICAs can be conveniently adjusted by selecting different starting materials. Taking all these advantages, we demonstrated their potency in the RFID tag antenna applications and in supporting LED chips. We expect them to find applications not only in conventional electronic packaging industry but also in the new areas which are featured of light weighted, low cost, wearable, and reconfigurable characters.

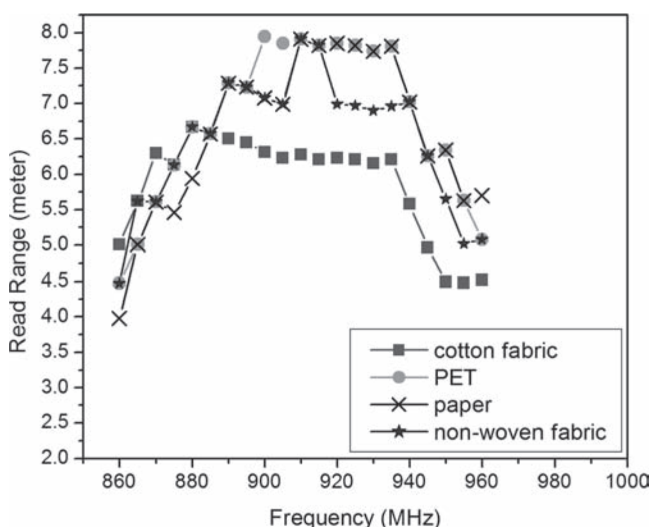

Figure 7. Read range testing results of the RFID tag samples prepared on four types of substrate materials, i.e. cotton fabric, PET film, paper, and non-woven fabric.

4. Experimental Section

Materials: Silver microflakes are from Chengdu Banknote printing complex and activated according to the method previously reported.[42] The average size of the silver microflakes was 5.6 micron. $NaBH_4$ (Aldrich) aqueous solution is added to the paste sample in various concentrations; then the paste is mixed in a THINKY AR250 mixer at 800 rpm for 2 minutes. Additional water is added to modulate the viscosity if in necessary. The pastes can be stored at room temperature over six months.

Preparation of the Water-Based PU: The 40 wt.% PU miniemulsion was prepared by the following procedures: 20 g (0.01 mol) poly(tetrahydrofuran)-2000 (PTHF-2000, Aldrich) and 2.68 g (0.02 mol) dimethylolpropionic acid (DMPA, Aldrich) were mixed with 13.34 g isophoron diisocyanate (IPDI, Aldrich) at 70 °C with the nitrogen protection. Dibutyltin dilaurate (DBTDL, Aldrich) 0.05 mL was added into the system for catalysis. After 2 hours, the temperature was lowered to 50 °C. Then 1.35 g (0.015 mol) 1, 4-butandiol was added into the system dropwise in half an hour. Following with adding 2.78 mL (0.02 mol) triethylamine (TEA) into the system for neutralization for half an hour and adding 68 mL water drop-by-drop into the system in 2 hours. The system was distilled under vacuum at 35 °C to remove the acetone for 2hrs. The transluscent miniemulsion with 40 wt% of the PU solid was acquired. The M_n of the polymer was 21×10^3 g/mol. Polydispersity was 1.32.

Characterizations: The WBICA thin films were printed onto a piece of DuPont Melinex PET film (~30 μm in thickness) using a DEK-260 screen printer at a printing speed of 250 mm/sec. The as-printed thin film is cured in a Memmert oven at 50 °C for 15 minutes for acceleration of cure. The thickness of the printed ICA samples is confirmed using a caliper and a Surface Profile System, Model Alpha-Step 200 (Tencor) to ensure the range is about 30 ± 5 μm.

FT-IR absorption of the pure solid PU thin film was carried out on a BioRad FTS 6000 ATR-FT-IR system, based on the transmittance mode (scanning range: 400 ~ 4000 cm^{-1}). The volume resistivity of the ICA samples was measured according to ASTM F1896-98. The samples were also conditioned in a TERCHY MHU-150L humidity chamber (85 °C/85% relative humidity) for 720 hours for the temperature-humidity testing (THT). The printed resistor samples with different filler content were aged for different time periods and their respective electrical resistivity was measured and compared with the result before the aging tests.

Raman spectra of Ag samples were obtained by using a LabRAM ARAMIS Raman confocal microscope (HORIBA Jobin Yvon) equipped with a 532 nm diode pumped solid state (DPSS) laser. Si wafer was used as the sample substrate for the measurements. The reduction treatment of the iodinated silver flakes was performed immediately after the iodination treatment of the silver flakes. Rhodamine 6G (10^{-7} M) aqueous solution was used as the probe molecule to evaluate the SERS activity of the silver flakes.

Supporting Information

Supporting Information is available from the Wiley Online Library or from the author.

© 2011 WILEY-VCH Verlag GmbH & Co. KGaA, Weinheim

FULL PAPER

Acknowledgements

The authors acknowledge the financial support from the Hong Kong government (Account No. 621810) and the start-up funding from the Shenzhen Graduate School, Tsinghua University.
Please note: This article was amended on December 6, 2011 to update the received date, which was incorrect in the version first published online.

Received: June 26, 2011
Revised: August 29, 2011
Published online: October 31, 2011

[1] H. Yan, Z. H. Chen, Y. Zheng, C. Newman, J. R. Quinn, F. Dotz, M. Kastler, A. Facchetti, *Nature* **2009**, *457*, 679.
[2] T. Sekitani, U. Zschieschang, H. Klauk, T. Someya, *Nat. Mater.* **2010**, *9*, 1015.
[3] U. Zschieschang, F. Ante, T. Yamamoto, K. Takimiya, H. Kuwabara, M. Ikeda, T. Sekitani, T. Someya, K. Kern, H. Klauk, *Adv. Mater.* **2010**, *22*, 982.
[4] B. D. Gates, *Science* **2009**, *323*, 1566.
[5] R. F. Service, *Science* **2004**, *304*, 675.
[6] R. Das, P. Harrop, Printed, Organic & Flexible Electronics Forecasts, Players & Opportunities 2009–2029 IDTechEx, **2009**; http://www.idtechex.com/research/reports/printed_organic_and_flexible_electronics_forecasts_players_and_opportunities_2009_2029_000219.asp (accessed October, 2011).
[7] C. Yang, H. Gu, W. Lin, M. M. F. Yuen, C. P. Wong, M. Xiong, B. Gao, *Adv. Mater.* **2011**, DOI: 10.1002/adma.201100530.
[8] B. Y. Ahn, E. B. Duoss, M. J. Motala, X. Y. Guo, S. I. Park, Y. J. Xiong, J. Yoon, R. G. Nuzzo, J. A. Rogers, J. A. Lewis, *Science* **2009**, *323*, 1590.
[9] S. R. Forrest, *Nature* **2004**, *428*, 911.
[10] B. Crone, A. Dodabalapur, Y. Y. Lin, R. W. Filas, Z. Bao, A. LaDuca, R. Sarpeshkar, H. E. Katz, W. Li, *Nature* **2000**, *403*, 521.
[11] S. De, T. M. Higgins, P. E. Lyons, E. M. Doherty, P. N. Nirmalraj, W. J. Blau, J. J. Boland, J. N. Coleman, *ACS Nano* **2009**, *3*, 1767.
[12] K. Y. Chun, Y. Oh, J. Rho, J. H. Ahn, Y. J. Kim, H. R. Choi, S. Baik, *Nat. Nanotechnol.* **2010**, *5*, 853.
[13] Z. B. Yu, Q. W. Zhang, L. Li, Q. Chen, X. F. Niu, J. Liu, Q. B. Pei, *Adv. Mater.* **2010**.
[14] T. Sekitani, T. Yokota, U. Zschieschang, H. Klauk, S. Bauer, K. Takeuchi, M. Takamiya, T. Sakurai, T. Someya, *Science* **2009**, *326*, 1516.
[15] S. I. Park, Y. J. Xiong, R. H. Kim, P. Elvikis, M. Meitl, D. H. Kim, J. Wu, J. Yoon, C. J. Yu, Z. J. Liu, Y. G. Huang, K. Hwang, P. Ferreira, X. L. Li, K. Choquette, J. A. Rogers, *Science* **2009**, *325*, 977.
[16] Z. Y. Fan, J. C. Ho, T. Takahashi, R. Yerushalmi, K. Takei, A. C. Ford, Y. L. Chueh, A. Javey, *Adv. Mater.* **2009**, *21*, 3730.
[17] Z. Y. Fan, H. Razavi, J. W. Do, A. Moriwaki, O. Ergen, Y. L. Chueh, P. W. Leu, J. C. Ho, T. Takahashi, L. A. Reichertz, S. Neale, K. Yu, M. Wu, J. W. Ager, A. Javey, *Nat. Mater.* **2009**, *8*, 648.
[18] J. Yoon, A. J. Baca, S. I. Park, P. Elvikis, J. B. Geddes, L. F. Li, R. H. Kim, J. L. Xiao, S. D. Wang, T. H. Kim, M. J. Motala, B. Y. Ahn, E. B. Duoss, J. A. Lewis, R. G. Nuzzo, P. M. Ferreira, Y. G. Huang, A. Rockett, J. A. Rogers, *Nat. Mater.* **2008**, *7*, 907.
[19] P. V. Nikitin, S. Lam, K. V. S. Rao, in *Antennas and Propagation Society International Symposium*, Vol. *2B*, **2005**, pp. 353.
[20] L. B. Hu, H. Wu, F. La Mantia, Y. A. Yang, Y. Cui, *ACS Nano 4*, 5843.
[21] L. B. Hu, J. W. Choi, Y. Yang, S. Jeong, F. La Mantia, L. F. Cui, Y. Cui, *Proc. Nat. Acad. Sci. USA* **2009**, *106*, 21490.
[22] T. Cohen-Karni, B. P. Timko, L. E. Weiss, C. M. Lieber, *Proc. Nat. Acad. Sci. USA* **2009**, *106*, 7309.
[23] A. C. Siegel, S. T. Phillips, M. D. Dickey, N. S. Lu, Z. G. Suo, G. M. Whitesides, *Adv. Funct. Mater.* **2010**, *20*, 28.
[24] T. Yamada, Y. Hayamizu, Y. Yamamoto, Y. Yomogida, A. Izadi-Najafabadi, D. N. Futaba, K. Hata, *Nat. Nanotechnol.* **2011**, *6*, 296.
[25] *The International Technology Roadmap for Semiconductors 2010 update*, **2010**, p. 74; http://www.itrs.net/(accessed October 2011).
[26] J. Liu, *Conductive Adhesives for Electronics Packaging*, Electrochemical Publications, Port Erin UK **1999**.
[27] Y. Li, K. S. Moon, C. P. Wong, *Science* **2005**, *308*, 1419.
[28] Y. Li, C. P. Wong, *Mater. Sci. Eng. R* **2006**, *51*, 1.
[29] Y. Li, C. P. Wong, *Soldering Surf. Mount Technol.* **2006**, *18*, 33.
[30] M. J. Yim, Y. Li, K. S. Moon, K. W. Paik, C. P. Wong, *J. Adhesion Sci. Technol.* **2008**, *22*, 1593.
[31] M. Andersen, P. Kiel, H. Larsen, J. Maxild, *Nature* **1978**, *276*, 391.
[32] A. Schaefer, T. J. Simat, *Food Addit. Contam.* **2004**, *21*, 390.
[33] C. Yang, Y. T. Xie, M. M. F. Yuen, B. Xu, B. Gao, X. M. Xiong, C. P. Wong, *Adv. Funct. Mater.* **2010**, *20*, 2580.
[34] H. J. Jiang, K. S. Moon, Y. Li, C. P. Wong, *Chem. Mater.* **2006**, *18*, 2969.
[35] D. Q. Lu, C. P. Wong, *Int. J. Adhesion Adhesives* **2000**, *20*, 189.
[36] R. W. Zhang, K. S. Moon, W. Lin, C. P. Wong, *J. Mater. Chem.* **2010**, *20*, 2018.
[37] C. Yang, M. M. F. Yuen, B. Xu, *US Provision patent No. 61/071,922*, US **2008**.
[38] C. Yang, B. Xu, M. M. F. Yuen, *The 58th IEEE Electronic Components and Technology Conference* **2008**, *5*, 213.
[39] R. W. Zhang, W. Lin, K. S. Moon, C. P. Wong, *ACS Appl. Mater. Interfaces* **2011**, *2*, 2637.
[40] Z. S. Petrovic, *Polym. Rev.* **2008**, *48*, 109.
[41] F. S. Guner, Y. Yagci, A. T. Erciyes, *Prog. Polym. Sci.* **2006**, *31*, 633.
[42] C. Yang, M. M. F. Yuen, B. Gao, Y. H. Ma, C. P. Wong, *J. Electron. Mater.* **2011**, *40*, 78.
[43] Y. Li, F. Xiao, C. P. Wong, *J. Polym. Sci., Part A: Polym. Chem.* **2007**, *45*, 181.
[44] M. Q. Yuan, S. H. Zhan, X. D. Zhou, Y. J. Liu, L. Feng, Y. Lin, Z. L. Zhang, J. M. Hu, *Langmuir* **2008**, *24*, 8707.
[45] Y. Li, K. Moon, C. P. Wong, in *IEEE CPMT International Symposium and Exhibition on Advanced Packaging Materials: Processes, Properties and Interfaces*, AtlantaGA, USA **2006**, pp. 179.
[46] S. Subramani, Y. J. Park, Y. S. Lee, J. H. Kim, *Prog. Org. Coatings* **2003**, *48*, 71.
[47] C. Yang, Y. H. Tang, W. M. Lam, W. W. Lu, P. Gao, C. B. Zhao, M. M. F. Yuen, *J. Mater. Sci.* **2010**, *45*, 3588.
[48] D. A. Wicks, Z. W. Wicks, *Prog. Org. Coatings* **2001**, *43*, 131.
[49] Q. B. Menga, S. Leeb, C. Nahc, Y. Leea, *Prog. Org. Coatings* **2009**, *66*, 382.
[50] V. Sharma, P. P. Kundu, *Prog. Polym. Sci.* **2008**, *33*, 1199.
[51] X. L. Li, Y. F. Wang, H. Y. Jia, W. Song, B. Zhao, *J. Raman Spectrosc.* **2005**, *36*, 635.
[52] R. W. Zhang, K. S. Moon, W. Lin, J. C. Agar, C. P. Wong, *Composites Sci. Technol.* **2011**, *71*, 528.
[53] C. Yang, Y. T. Xie, M. M. F. Yuen, X. M. Xiong, C. P. Wong, *Phys. Chem. Chem. Phys.* **2010**, *12*, 14459.
[54] P. Hildebrandt, M. Stockburger, *J. Phys. Chem.* **1984**, *88*, 5935.
[55] S. Yamamoto, K. Fujiwara, H. Watarai, *Anal. Sci.* **2004**, *20*, 1347.
[56] M. Moskovits, J. S. Suh, *J. Am. Chem. Soc.* **1985**, *107*, 6826.
[57] D. Lu, C. P. Wong, *J. Thermal Anal. Calorimetry* **2000**, *59*, 729.
[58] S. M. Nie, S. R. Emery, *Science* **1997**, *275*, 1102.
[59] F. J. GarciaVidal, J. B. Pendry, *Phys. Rev. Lett.* **1996**, *77*, 1163.
[60] A. M. Michaels, J. Jiang, L. Brus, *J. Phys. Chem. B* **2000**, *104*, 11965.
[61] D. Li, D. Sutton, A. Burgess, D. Graham, P. D. Calvert, *J. Mater. Chem.* **2009**, *19*, 3719.
[62] P. Kumar, H. W. Reinitz, J. Simunovic, K. P. Sandeep, P. D. Franzon, *Food Sci.* **2009**, *74*, R101.
[63] K. Finkenzeller, *RFID-Handbuch*, *Vol. 3. akt. und erw.*, Hanser-Verlag, München, **2002**.

© 2011 WILEY-VCH Verlag GmbH & Co. KGaA, Weinheim